Original Article

MOLECULAR METABOLISM

A novel lncRNA RP11-386G11.10 reprograms lipid metabolism to promote hepatocellular carcinoma progression

Kequan Xu [1,2,3], Peng Xia [1,2,3], Xiangdong Gongye [1,2,3], Xiao Zhang [1,2], Shuxian Ma [1,2], Zhang Chen [1,2], Hao Zhang [1,2], Jie Liu [1,2], Yingyi Liu [1,2], Yonghua Guo [1,2], Ye Yao [1,2], Meng Gao [1,2], Yiran Chen [1,2], Zhonglin Zhang [1,2,], Yufeng Yuan [1,2,*]**

ABSTRACT

Objective: Emerging studies suggest that long non-coding RNAs (lncRNAs) play crucial roles in hepatocellular carcinoma (HCC). A rapidly increasing number of studies have shown that metabolic changes including lipid metabolic reprogramming play a significant role in the progression of HCC. But it remains to be elucidated how lncRNAs affect tumor cell metabolism.

Methods: Through analysis and screening of The Cancer Genome Atlas-Liver Hepatocellular Carcinoma (TCGA-LIHC) dataset, we found a novel lncRNA RP11-386G11.10 was overexpressed, related to prognosis, conserved and non-protein-coding in HCC and related to poor prognosis. Then, CCK-8, colony formation, Transwell invasion, wound healing assays were performed and nude mouse subcutaneous tumour formation and lung metastasis models were established to explore the effect of RP11-386G11.10 on HCC tumour growth and metastasis. Chromatography-mass spectrometry (GC-MS) and Nile red staining detected the effect of RP11-386G11.10 on lipid metabolism in HCC. Mechanistically, we clarified the RP11-386G11.10/miR-345-3p/HNRNPU signalling pathway through dual luciferase reporter, RNA immunoprecipitation (RIP) and chromatin immunoprecipitation (ChIP) assays and identified ZBTB7A as a transcription factor of RP11-386G11.10.

Results: RP11-386G11.10 was overexpressed in HCC and positively correlated with tumour size, TNM stage, and poor prognosis in HCC patients. RP11-386G11.10 promoted the proliferation and metastasis of HCC cells in vitro and in vivo. Mechanistically, RP11-386G11.10 acted as a competing endogenous RNA (ceRNA) for miR-345-3p to regulate the expression of HNRNPU and its downstream lipogenic enzymes, leading to lipid accumulation in HCC cells and promoting their growth and metastasis. In addition, we identified ZBTB7A as a transcription factor of RP11-386G11.10. Moreover, HNRNPU promoted the expression of ZBTB7A in HCC cells, thereby increasing the transcriptional activity of RP11-386G11.10, and forming a positive feedback loop, ultimately leading continuous lipid accumulation, growth and metastasis in HCC cells.

Conclusions: Our results indicated that the lncRNA RP11-386G11.10 was a novel oncogenic lncRNA that was strongly correlated with the poor prognosis of HCC. The ZBTB7A-RP11-386G11.10-HNRNPU positive feedback loop promoted the progression of HCC by regulating lipid anabolism. RP11-386G11.10 may become a new diagnostic and prognostic biomarker and therapy target for HCC.

© 2022 The Author(s). Published by Elsevier GmbH. This is an open access article under the CC BY-NC-ND license (http://creativecommons.org/licenses/by-nc-nd/4.0/).

Keywords Hepatocellular carcinoma; RP11-386G11.10; HNRNPU; ZBTB7A; Lipid metabolism

1. INTRODUCTION

Hepatocellular carcinoma (HCC) is a highly malignant solid tumour, and its morbidity and mortality are among the highest of all cancers [1]. Although there are many immunotherapies and targeted therapiesfor HCC, the overall prognosis of HCC patients is still poor, and the postoperative recurrence and metastasis rates remain high [2–4]. Therefore, it is necessary to further explicate the biological mechanisms of HCC in order to develop novel effective therapeutic strategies. Long noncoding RNAs (lncRNAs) are noncoding RNAs with a length of more than 200 bases [5]. Reports have indicated that most lncRNAs perform their functions by acting as molecular sponges for miRNAs

[1]Department of Hepatobiliary & Pancreatic Surgery, Zhongnan Hospital of Wuhan University, Wuhan, 430071, PR China [2]Clinical Medicine Research Center for Minimally Invasive Procedure of Hepatobiliary & Pancreatic Diseases of Hubei Province, Hubei, PR China

[3] These authors contributed equally to this work.

*Corresponding author. Department of Hepatobiliary & Pancreatic Surgery, Zhongnan Hospital of Wuhan University, Wuhan, 430071, PR China.

**Corresponding author. Department of Hepatobiliary & Pancreatic Surgery, Zhongnan Hospital of Wuhan University, Wuhan, 430071, PR China.

E-mails: surexkq1998@163.com (K. Xu), Qazwsx1573@126.com (P. Xia), gyxd97@163.com (X. Gongye), 592579412@qq.com (X. Zhang), 2018305231095@whu.edu.cn (S. Ma), cz2482108839@163.com (Z. Chen), zhanghao370123@163.com (H. Zhang), liuj_0313@163.com (J. Liu), 2013302180342@whu.edu.cn (Y. Liu), yonghuaguo@whu.edu.cn (Y. Guo), 724153986@qq.com (Y. Yao), gaomeng970228@163.com (M. Gao), 2015302180114@whu.edu.cn (Y. Chen), zhonglinzhang@whu.edu.cn (Z. Zhang), yuanyf1971@whu.edu.cn (Y. Yuan).

Received April 16, 2022 • Revision received June 11, 2022 • Accepted June 27, 2022 • Available online 5 July 2022

https://doi.org/10.1016/j.molmet.2022.101540

 © 2022 The Author(s). Published by Elsevier GmbH. This is an open access article under the CC BY-NC-ND license (http://creativecommons.org/licenses/by-nc-nd/4.0/).

[6,7]. And mir-345-3p, is a common tumor suppressor as molecular sponges for lncRNAs [8,9]. Through this mechanism, lncRNAs regulate the key genes with specific functions, thereby affecting the proliferation and metastasis of tumour cells [10]. But the function of many lncRNAs has not yet been reported.

Recent studies have shown that metabolic reprogramming is considered a hallmark of cancer, especially in the liver, which is considered the "central organ" of systemic metabolism [11]. Separate from the typical changes resulting from the Warburg effect, lipid metabolic reprogramming plays a pivotal role in the development of HCC, and abnormal lipid metabolism promotes HCC occurrence and development. In addition, abnormal lipid anabolism is an indicator of malignant tumour progression [12]. Recent studies have shown that the enhancement of lipid synthesis promotes the progression of nonalcoholic fatty liver disease (NAFLD) [13,14], as well as the growth and metastasis of HCC cells [15–17]. These findings strongly indicate that the increase in lipid synthesis is the driving force supporting the progression of HCC, but the specific mechanism still needs further investigation.

HNRNPU is a multifunctional protein that regulates the precursor mRNA splicing through splicing decisions mediated by direct binding to target genes or by protein/protein interaction-mediated splicing decisions [18]. HNRNPU is a nucleoprotein, but it can bind to the nuclear matrix to help locate genes and proteins (including nuclear transcription factors) [19,20]. The latest research indicates that HNRNPU promotes the proliferation, invasion and metastasis of HCC cells and promotes the expression of lipogenic enzymes such as FASN [18,21,22].

ZBTB7A, also known as Pokemon, is a transcription factor involved in the development of various tumors [23]. Its polypeptide chain is composed of 584 amino acid residues and folds in an N-terminal POZ/BTB domain and a C-terminal domain containing four zinc-finger motifs and a nuclear localization signal. ZBTB7A is overexpressed in several tumors and contributes to the development of hepatocellular carcinoma [23]. And recent studies have reported that ZBTB7A promotes the progression of HCC and regulates lipid anabolism [24,25].

In this study, we identified an oncogenic novel lncRNA, RP11-386G11.10, in HCC through analysis of The Cancer Genome Atlas-Liver Hepatocellular Carcinoma (TCGA-LIHC) dataset and 80 samples from Zhongnan Hospital of Wuhan University. Our results indicate that the ZBTB7A/RP11-386G11.10/miR-345-3p/HNRNPU axis reprograms lipid metabolism, enhances the expression of lipogenic enzymes, and forms a positive feedback loop for HNRNPU-ZBTB7A to promote lipid synthesis. In summary, our results clarify that RP11-386G11.10 promotes the progression of HCC and regulates lipid metabolic reprogramming in HCC via a previously unrecognized way.

2. MATERIALS AND METHODS

2.1. Tissue sample

Between October 2015 and September 2020, 80 pairs of HCC tissues and matched nontumour tissues were collected with written informed consent from HCC patients in Zhongnan Hospital of Wuhan University (Hubei, China). None of the patients enrolled in this study received preoperative chemotherapy or radiotherapy. Two pathologists confirmed the HCC diagnosis. This study was conducted in accordance with the Declaration of Helsinki and was approved by the Ethics Committee of Zhongnan Hospital of Wuhan University (KELUN 2018010).

2.2. Bioinformatics analysis

In our study, we obtained HCC patient information from the TCGA dataset. We used Gene Set Enrichment Analysis (GSEA) v3.0 software and FunRich for gene enrichment analysis and Gene ontology (GO) analysis, respectively. The URLs of all online analysis websites are listed in Table S3.

2.3. Cell culture

Human HCC cells (HepG2, Hep3B, Li7, Huh-7, HCC-LM3 and Hep-G2) were originally purchased from the Cell Bank of the Chinese Academy of Sciences (Shanghai, China). Normal liver cells (L02) were originally purchased from Fuxiang Biotechnology Company (Shanghai, China). L02, Huh-7, HCC-LM3, and Hep-G2 cell lines were cultured in DMEM medium plus 10% fetal bovine serum (FBS). Hep-3B cell lines were cultured in MEM medium plus 10% FBS, 1% non-essential amino acids, and 1% sodium pyruvate. Li-7 cell lines were cultured in MEM medium plus 10% FBS. All cell lines maintained in a 5% CO2 incubator at 37 °C [26].

2.4. RNA extraction and real-time quantitative PCR (qRT-PCR)

Total RNA was extracted with TRIzol (T9108, Takara, Dalian, China) and reverse transcribed using an enzyme kit. Then, 2 × ChamQ Universal SYBR qPCR Master Mix (Q711-02, Vazyme, Nanjing, China) was used for qRT-PCR. The sequences of all PCR primers used are listed in Table S2.

2.5. Western blot analysis

Total protein was extracted with RIPA buffer (R0010, Solarbio, Beijing, China). Protein extracts were transferred to PVDF membranes and incubated with the appropriate antibodies. All antibodies used are listed in Table S3. An ECL imaging system (Tanon-5200, Shanghai, China) was used for the detection of ECL signals.

2.6. Immunohistochemical (IHC) and immunofluorescence (IF) analysis

For IHC analysis, the paraffin sections were placed in an oven at 65 °C for 2 h, dewaxed to water, and washed three times with PBS for 5 min each time. The sections were microwaved in EDTA buffer, and the power was turned off after medium heat to boiling, and the low heat to boiling was carried out at intervals of 10 min. After natural cooling, wash sections with PBS. Sections were placed in 3% hydrogen peroxide solution and incubated at room temperature for 10 min in the dark. Then block sections with 5% BSA for 20 min after drying. Remove the BSA solution, add about 50 μl of diluted primary antibody to each section to cover the tissue, and keep overnight at 4 °C. After washing sections with PBS 3 times, 5 min each time, add 50 μl—100 μl of the secondary antibody of the corresponding species (see Appendix 2) to each section, and incubate at 37 °C for 50 min. Then add 50—100 μl of freshly prepared DAB solution to each section, and control the color development under the microscope. After completing color development, sections were rinsed with distilled water or tap water, counterstained with hematoxylin, differentiated with 1% hydrochloric acid alcohol (about 1s), rinsed with tap water, returned to blue with ammonia, and rinsed with running water. Sections were subjected to gradient alcohol 75%, 90%, 100%, and 100% for 10 min each, dehydrated and dried, transparent in xylene, and mounted with neutral gum.

For IF analysis, cells were washed three times with phosphate-buffered saline (PBS) and fixed with 4% paraformaldehyde for 20 min. HCC cells were then permeabilized with 0.5% NP-40 in PBS for 20 min and blocked with 5% bovine serum albumin for a duration of 30 min. Next, cells were incubated with primary antibodies for 2 h and incubated with secondary antibodies for 1 h. For the nuclei, cells were stained with DAPI (D1306, Thermo Fisher, Shanghai, China). Finally,

 © 2022 The Author(s). Published by Elsevier GmbH. This is an open access article under the CC BY-NC-ND license (http://creativecommons.org/licenses/by-nc-nd/4.0/).

confocal microscopy (IX51, OLYMPUS, Japan) was used for image acquisition [26].

2.7. Plasmids, siRNA transfection and shRNA transduction

Lipo3000 (L3000008, Thermo Fisher, Shanghai, China) and a pcDNA 3.1 vector containing the coding sequence of RP11-386G11.10 were cotransfected into the HCC cells. The siRNA against zinc finger and BTB domain containing 7A (ZBTB7A) was designed and synthesized by Qingke Biological and delivered into HCC cells with GenMuteTM (SL100568, SignaGen, USA). Lentiviruses were packaged with the shRNA or negative control construct by Gene Create Co. (Wuhan, China). HCC cells were incubated with 2 μg/mL puromycin to generate cell lines with stable RP11-386G11.10 knockdown. The siRNA and shRNA sequences used are listed in Table S2.

2.8. Xenograft model and in vivo metastasis model in nude mice

We ordered five-week-old male BALB/c nude mice from the Laboratory Animal Center of Wuhan University (Wuhan, China). HCC-LM3 cells transfected with RP11-386G11.10-sh2, miR-345-3p mimics, RP11-386G11.10-sh2 + miR-345-3p inhibitors or RP11-386G11.10-sh2 + HNRNPU plasmid were injected subcutaneously into the left axillary vein, tail vein or spleen capsule of these mice. Additionally, we used g418 to screen for stable miR-345-3p overexpression or knockdown cells, which were injected every week for 3 continuous weeks to ensure transfection efficiency in vivo. Subcutaneous tumours were collected 20 days later, while in vivo metastasis samples were collected after 6 weeks. In vivo analysis of the xenografts and in vivo metastasis were conducted as previously described [26]. All experimental procedures involving animals used in this study were reviewed and approved by the Institutional Animal Care and Use Committee (IACUC) of the Wuhan University Center for Animal Experiment and performed in accordance with the Guidelines for the Care and Use of Laboratory Animals of the Chinese Animal Welfare Committee.

2.9. Cell proliferation, migration and invasion assays

As previously described, CCK-8 and colony formation assays were used to evaluate cell proliferation [26]. A wound-healing assay was used to evaluate cell migration [26]. A Transwell invasion assay was used to determine cell invasion [26].

2.10. Reporter plasmid construction and luciferase reporter detection

The wild-type (WT) and mutant (MUT) binding site sequences in RP11-386G11.10 or in the 3′-UTR of heterogeneous nuclear ribonucleoprotein U(HNRNPU) with miR-345−3p, ZBTB7A and RP11-386G11.10 promoter region and insert it into pGL3 basic vector. The resulting constructs were named RP11-386G11.10-WT/Mut, HNRNPU-3′-UTR-WT/Mut and RP11-386G11.10-promoter-WT/Mut. After 48 h of transfection with Lipofectamine 3000, luciferase activity was measured with a Dual Luciferase® Reporter Assay System (E1910, Promega, Shanghai, China).

2.11. Chromatin immunoprecipitation (ChIP)

The potential binding between ZBTB7A and the RP11-386G11.10 promoter regions was evaluated in HCC cells by ChIP as previously described [26]. Briefly, cells were crosslinked with formaldehyde and sonicated to an average length of 200−1000 bp. Immunoprecipitation was conducted with an anti-ZBTB7A antibody or IgG control. qRT-PCR analysis was performed to measure the relative enrichment of target genes. All primer sequences and antibody used are listed in Table S2.

2.12. RNA immunoprecipitation (RIP)

Protein-RNA interactions were identified using RNA immunoprecipitation analysis. Pierce™ Magnetic RNA-Protein Pull-Down Kit (20164, Thermo Fisher, Shanghai, China) was used for RIP analysis. The cells were collected and completely lysed in RIP lysis buffer following the manufacturer's instructions. Next, RIP Lysate was incubated with human anti-Argonaute2 (Ago2) antibody magnetic beads (HY−K0202, MedChemExpress, Shanghai, China) or anti-mouse IgG negative control magnetic beads (HY−K0202, MedChemExpress, Shanghai, China). RNA bound with magnetic beads was extracted and verified by qRT-PCR [26].

2.12.1. Fluorescence in situ hybridization (FISH)

The RP11-386G11.10 probe was designed and produced by AXL-bio (Guangzhou, China). Cells were cultured in 6-well plates overnight and then fixed with 4% paraformaldehyde for 30 min before treatment with 0.5% Triton X-100 for 20 min. After washing with 2 × SSC for 10 min, the cells were incubated with the RP11-386G11.10 probe (sequence: 5′-GTCCTCCATCACTGCTTCCCTGAGATTTGATGGAGCCCT GAATGTTGACCT-3′) and then with anti-digoxigenin-fluorescein-Fab fragments (Roche Diagnostics, Indianapolis, IN, USA). The slides were mounted with ProLong Gold Antifade Reagent and detected with DAPI (D1306, Thermo Fisher, Shanghai, China). RP11-386G11.10 was observed under an Olympus FluoView™ FV1000 confocal microscope (Olympus, Hamburg, Germany) [26].

2.12.2. Nucleocytoplasmic RNA fractionation analysis

Nuclear and cytoplasmic RNAs used to qRT-PCR reverse transcription and were extracted and purified using the Cytoplasmic & Nuclear RNA Purification Kit (NGB-21000, Norgen, Belmont, CA), followed by qRT-PCR analysis. U6 and GAPDH were used as nuclear and cytoplasmic internal reference, respectively.

2.12.3. Gas chromatography-mass spectrometry (GC−MS)

Equal number of cultured tumour cells (about 1 × 107 cells) were collected and subjected to fatty acids extraction. The extract was injected into GC−MS (Agilent 7890B, Agilent Technologies, USA) containing a DB-WAX capillary column for fatty acids detection. GC−MS and the statistical analysis were performed according to the instructions by Shanghai Applied Protein Technology [27].

2.12.4. RNA-sequencing (RNA-seq)

Agilent 2100 was used to assess RNA integrity. VAHTS mRNA-seq v2 Library Prep Kit (NR602-01, Vazyme, Nanjing, China) for Illumina was used to generate Sequencing libraries. And the libraries were sequenced on an Illumina NovaSeq platform. Differentially expressed genes were defined as P-value < 0.05 and absolute log2 fold change >1.

2.13. Triglyceride and cholesterol assays

Intracellular and intratumoural triglyceride and cholesterol contents were assayed using triglyceride assay kit (E1013-105, Applygen Technologies Inc, Beijing, China) and cholesterol assay kit (E1015-105, Applygen Technologies Inc, Beijing, China) according to the manufacturer's recommended protocols [28].

2.14. Nile Red staining

Cultured cells were fixed with 4% paraformaldehyde solution in 6-well plates, and washed in 1 × PBS prior to staining with Nile Red solution (7385-67-3, Solarbio, Beijing, China) diluted 1:100 with PBS for 20 min in the dark. Samples were then washed twice with PBS, and stained with DAPI. Images were acquired by IF microscopy. Tissues

 © 2022 The Author(s). Published by Elsevier GmbH. This is an open access article under the CC BY-NC-ND license (http://creativecommons.org/licenses/by-nc-nd/4.0/).

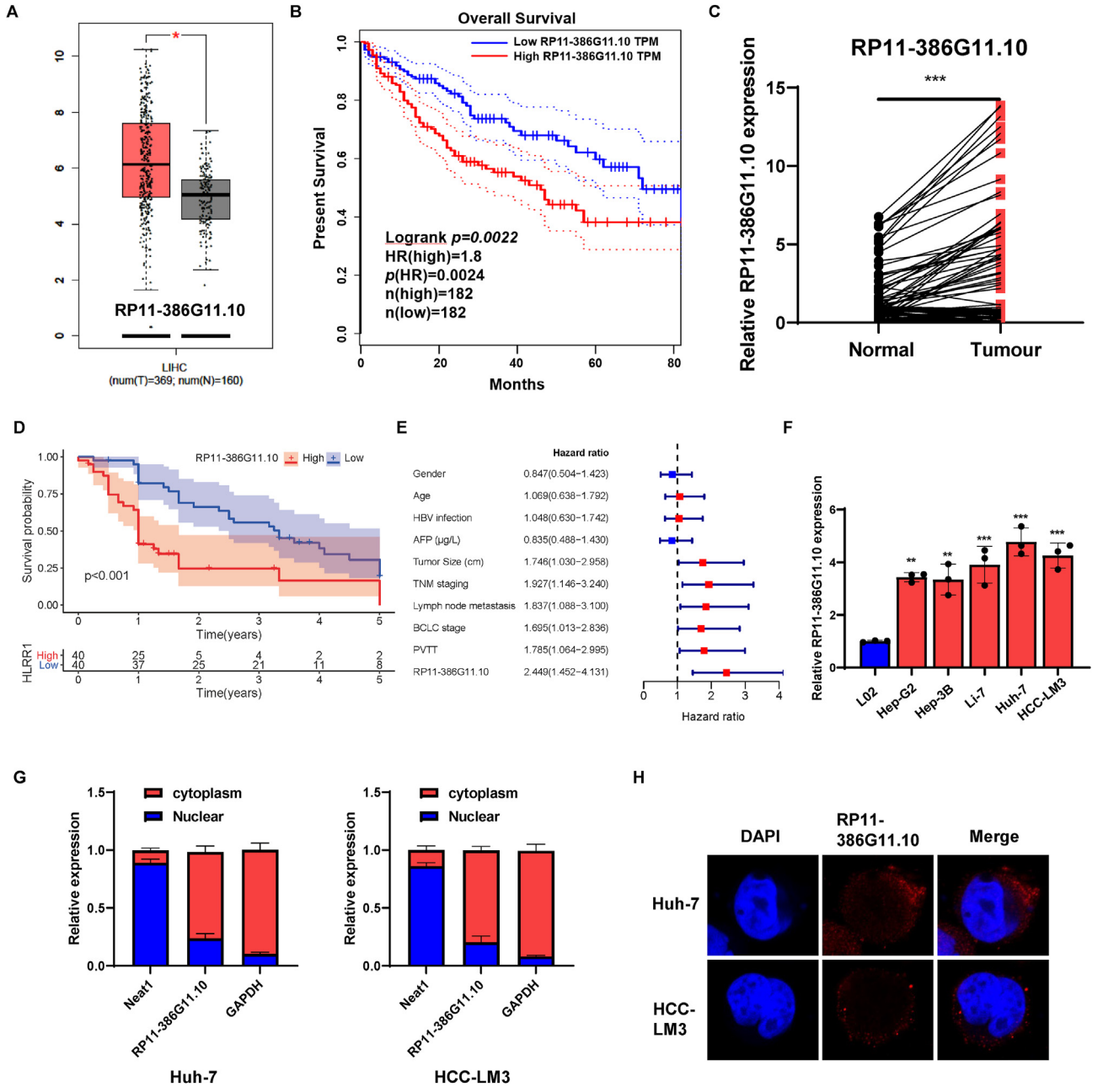

Figure 1: RP11-386G11.10 expression is significantly increased in HCC. **A** HCC and non-tumor tissue RP11-386G11.10 transcription levels based on the analysis of TCGA-LIHC data set. **B** Overall survival curves of HCC patients based on RP11-386G11.10 expression. **C** The expression of RP11-386G11.10 in 80 pairs of HCC tissues and its paired non-tumor tissues. **D** 80 cases of HCC patients based on the overall survival curve of RP11-386G11.10 expression. **E** The hazard ratio analysis of clinicopathological factors in 80 HCC patients. **F** RP11-386G11.10 expression in hepatocytes and HCC cell lines. **G, H** The main position of RP11-386G11.10 analyzed by the nuclear-cytoplasmic RNA fractionation and FISH experiments. $*p < 0.05$, $**p < 0.01$, $***p < 0.001$.

were cryosectioned, and a histochemical pen was used to draw a circle around the tissue to prevent the incubation solution from flowing away in subsequent processing. The other steps for Nile Red staining of tissues were the same as those used for cells.

2.15. Metabolic assays

Cells were seeded in 6-well plate and cultured for 24 h, then culture medium was collected and glucose and lactate were examined by glucose assay kit (F006-1-1, Jiancheng Bioengineering Institute, Nanjing, China) and lactate assay kit (A019-2-1, Jiancheng Bioengineering Institute, Nanjing, China) respectively. For intracellular ATP measurement, cells were collected and ATP assay kit (A095-1-1, Jiancheng Bioengineering Institute, Nanjing, China) was applied according to manufacturer's protocol. Results were normalized by protein concentration and triple independent experiments were performed.

The rate of metabolic flux was determined by seahorse XFp extracellular flux analyzer (Agilent Technologies, Santa Clara, CA, USA).

 © 2022 The Author(s). Published by Elsevier GmbH. This is an open access article under the CC BY-NC-ND license (http://creativecommons.org/licenses/by-nc-nd/4.0/).

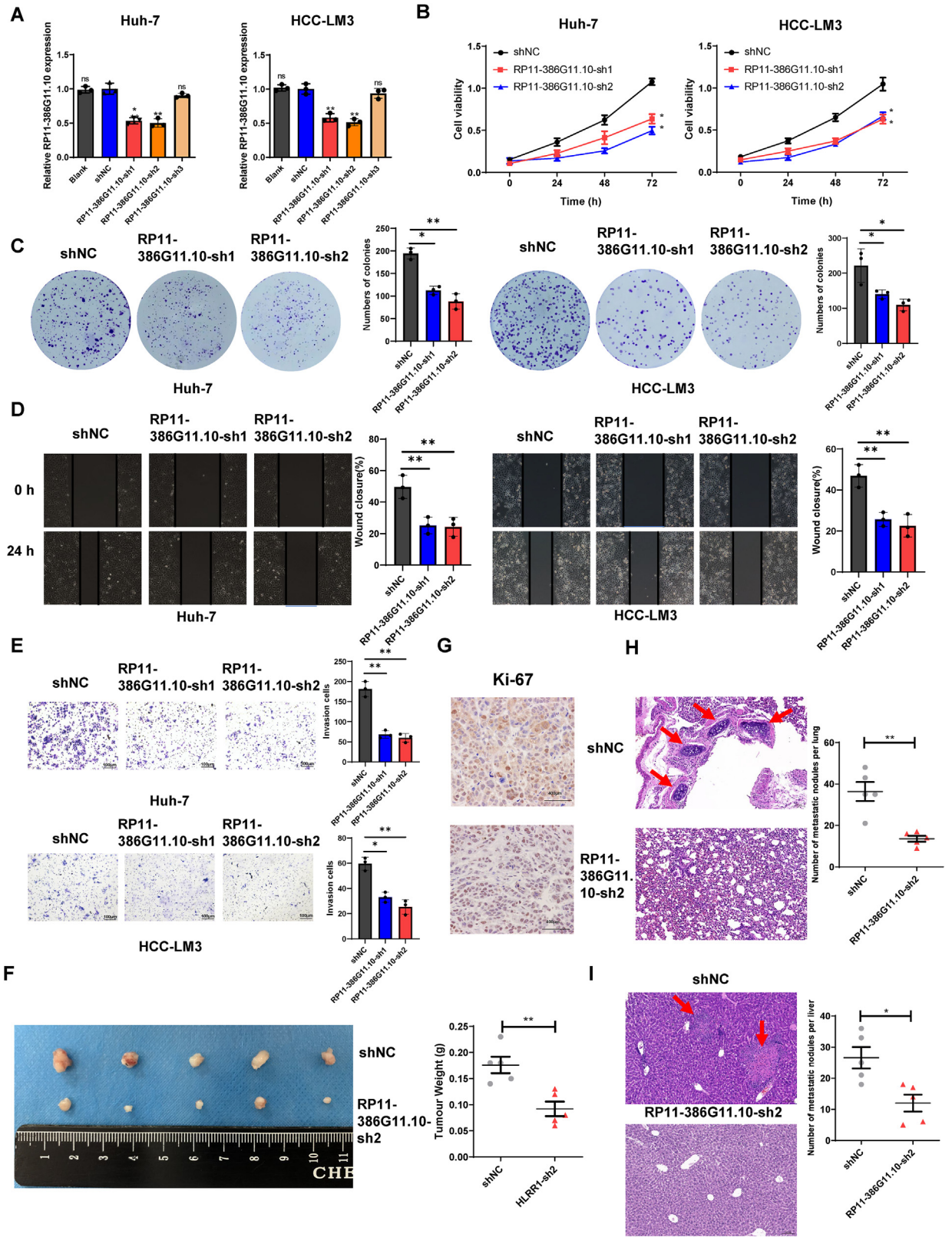

Figure 2: RP11-386G11.10 promotes HCC proliferation and metastasis. **A** Expression of RP11-386G11.10 in Huh-7 and HCC-LM3 cells transfected with shNC and RP11-386G11.10 targeting shRNA (shHRLL1). **B, C** CCK-8 and colony formation assay showed the proliferation ability of Huh-7 and HCC-LM3 cells. **D** Scratch wound-healing assay showed the migration ability of cells. **E** Transwell Matrigel invasion assay showed the cell invasion ability. **F** A xenograft model established from control or stable RP11-386G11.10 knockdown HCC-LM3 cells, and evaluate the weight of the anatomical tumor. **G** The expression of Ki-67 was determined by IHC analysis. **H, I** The metastasis in the lungs and livers of nude mice injected with shNC or RP11-386G11.10-sh2 HCC cells. Magnification, 100 $\times$. $^{*}p < 0.05$, $^{**}p < 0.01$, $^{***}p < 0.001$.

 © 2022 The Author(s). Published by Elsevier GmbH. This is an open access article under the CC BY-NC-ND license (http://creativecommons.org/licenses/by-nc-nd/4.0/).

Cells were seeded in Seahorse XFp cell culture plates and allowed to adhere overnight. Then the medium was replaced with substrate-limited medium for 16 h. Briefly, cells were seeded at a density of 4×10^4 cells per well in medium supplemented with 2 mM glutamine (for ECAR), 2 mM glutamine, 10 mM glucose and 1 mM pyruvate (for OCR), or 111 mM NaCl, 4.7 mM KCl, 1.25 mM CaCl2, 2 mM MgSO4, 1.2 mM NaH2PO4, supplemented with 2.5 mM Glucose, 0.5 mM carnitine and 5 mM HEPES (for FAO). After the equilibration of temperature and pH, measurements were recorded with the analyser according to the manufacturer's protocol.

2.16. Actinomycin D chase assay

Actinomycin D (Act D) chase assay was performed for mRNA stability as previously described [26].

2.17. Statistical analysis

Data were analysed using Prism 8.0 (GraphPad Software, La Jolla, CA, USA) and SPSS 21.0 (IBM SPSS Statistics for Windows, version 21.0. Armonk, NY, USA: IBM Corp). Student's t-test was used for comparisons between the two groups, and the Kaplan—Meier method was used for survival analysis. The data obtained from the CCK-8 assay and xenograft growth experiment were evaluated by two-sided unpaired t-test. Correlations between gene expression levels were evaluated using Pearson correlation analysis. All data meet the assumptions of the tests, and the variance is similar between the groups that are being statistically compared. All experiments were repeated three times, and $P < 0.05$ was considered statistically significant for all experiments.

3. RESULTS

3.1. The lncRNA RP11-386G11.10 is significantly upregulated in HCC tissues and cell lines

To explore the role of HCC-related lncRNAs, we screened the TCGA database and identified a novel lncRNA RP11-386G11.10 (ENSG00000258017.1, located on chromosome 12:49,521,565—49,541,652), which is overexpressed in all types of cancer and cancer cell lines, and related to prognosis, conserved and non-protein-coding in HCC (Fig. S1A—C). We generated a Kaplan -Meier survival curve, and found that patients with high RP11-386G11.10 expression had a poor prognosis (Figure 1A, Figure 1B). QRT-PCR analysis of 80 pairs of HCC and nontumour tissues and survival analysis of patients stratified by RP11-386G11.10 expression (Cutoff-High/Low = 0.5) confirmed this finding (Figure 1C, Figure 1D). In addition, one-way analysis of variance showed that RP11-386G11.10 expression in HCC tissues was positively correlated with poor prognosis, as well as tumour size, TNM stage, lymph node metastasis, Barcelona Clinic Liver Cancer (BCLC) stage and portal vein tumour thrombosis (PVTT) (Figure 1E). Bioinformatics analysis based on the UCSC Genome Browser database and the Coding Potential Calculator 2(CPC2) tool showed that RP11-386G11.10 is conserved and non-protein-coding (Figure 1D, Fig. S1E). And we used 5′- and 3′-RACE analyses to obtain the full length of RP11-386G11.10 (Fig. S1F). Next, RP11-386G11.10 mRNA levels were found to be upregulated in HCC cells (HepG2, Hep3B, Li7, Huh-7 and HCC-LM3)compared with L02 normal human hepatocytes and were the most upregulated in Huh-7 and HCC-LM3 cells (Figure 1F). Additionally, the nucleocytoplasmic RNA fractionation and FISH results showed that RP11-386G11.10 is localized mainly in the cytoplasm (Figure 1G, Figure 1H). Our results indicated that the lncRNA RP11-386G11.10 is upregulated in HCC, and that this upregulation may be related to the progression of HCC.

3.2. The lncRNA RP11-386G11.10 promotes HCC cell proliferation and metastasis in vivo and in vitro

To further clarify the biological function of RP11-386G11.10, we used the Huh-7 and HCC-LM3 cell lines to establish a knockdown model (Figure 2A). Cell proliferation assays showed that RP11-386G11.10 knockdown significantly inhibited the proliferation of HCC cells (Figure 2B, Figure 2C). The Transwell invasion assay and wound healing assay results showed that knocking down RP11-386G11.10 significantly reduced the invasion and migration abilities of HCC cells (Figure 2D, Figure 2E). And RP11-386G11.10 overexpression increased cell proliferation, invasion, and migration (Figs. S2A—E). To further explore the role of RP11-386G11.10 in vivo, we injected shNC or RP11-386G11.10-sh2 HCC-LM3 cells subcutaneously into BALB/c nude mice. The tumour volumes and weights in the RP11-386G11.10-sh2 group were significantly reduced compared with those in the shNC group (Figure 2F). In addition, the IHC results showed that knocking down RP11-386G11.10 significantly reduced the expression of ki-67 (Figure 2G). We also established an in vivo metastasis model and found that the RP11-386G11.10-sh2 group had fewer lung and liver metastatic nodules (Figure 2H,I). In summary, compared with shNC, this lncRNA promoted the proliferation and metastasis of HCC cells in vivo and in vitro.

3.3. The lncRNA RP11-386G11.10 promotes HCC development and increases de novo lipid synthesis in HCC

To thoroughly investigate the mechanism by which RP11-386G11.10 regulates the occurrence and development of HCC, we performed RNA-seq to identify potential genes following RP11-386G11.10 knockdown in Huh-7 cells. RNA-seq data showed that RP11-386G11.10 knockdown resulted in differential expression of a total of 687 genes, including 477 up-regulated genes and 210 down-regulated genes (Figure 3A). The heatmap showed the expression of all differentially expressed genes in each sample (Figure 3B). The Kyoto Encyclopedia of Genes and Genomes (KEGG) pathway analysis showed that the fatty acid metabolism signaling pathway was one of the most significantly enriched pathways (Figure 3C). Then we downloaded the TCGA-LIHC dataset for GESA and found the genes coexpressed with RP11-386G11.10 were significantly enriched in fatty acid (FA) metabolism (Figure 3D). Since abnormal lipid metabolism is thought to be related to the progression of HCC, we evaluated whether RP11-386G11.10 affects lipid metabolism in HCC cells. The levels of triglycerides and cholesterol in HCC cells with RP11-386G11.10 knockdown were significantly reduced compared with those in control cells (Figure 3E). Gas chromatography—mass spectrometry (GC—MS) results showed that the contents of intracellular FAs, such as palmitic acid (C16:0), palmitoleic acid (C16:1), stearic acid (C18:0) and oleic acid (C18:1), were significantly reduced by RP11-386G11.10 knockdown (Figure 3F). Moreover, as shown by Nile Red staining, RP11-386G11.10 knockdown inhibited intracellular lipid accumulation (Figure 3G). Next, we determined the mechanism by which RP11-386G11.10 regulates abnormal lipid metabolism in HCC cells. We examined the mRNA levels of lipid metabolism genes in 80 HCC tissue samples. Pearson correlation analysis showed that the mRNA levels of some lipid metabolism genes, including the lipogenic enzyme fatty acid synthase (FASN) ($r = 0.29$, $p = 0.0088$), ATP-citrate lyase (ACLY) ($r = 0.26$, $p = 0.0220$), acetyl-CoA carboxylase (ACC) ($r = 0.28$, $p = 0.0106$) and stearoyl-CoA desaturase (SCD) ($r = 0.27$, $p = 0.0129$) had significant correlations with that of RP11-386G11.10 (Figure 3H). The qRT-PCR and western bolt results showed that knocking down RP11-386G11.10 reduced the expression of key lipid synthesis genes such

 © 2022 The Author(s). Published by Elsevier GmbH. This is an open access article under the CC BY-NC-ND license (http://creativecommons.org/licenses/by-nc-nd/4.0/).

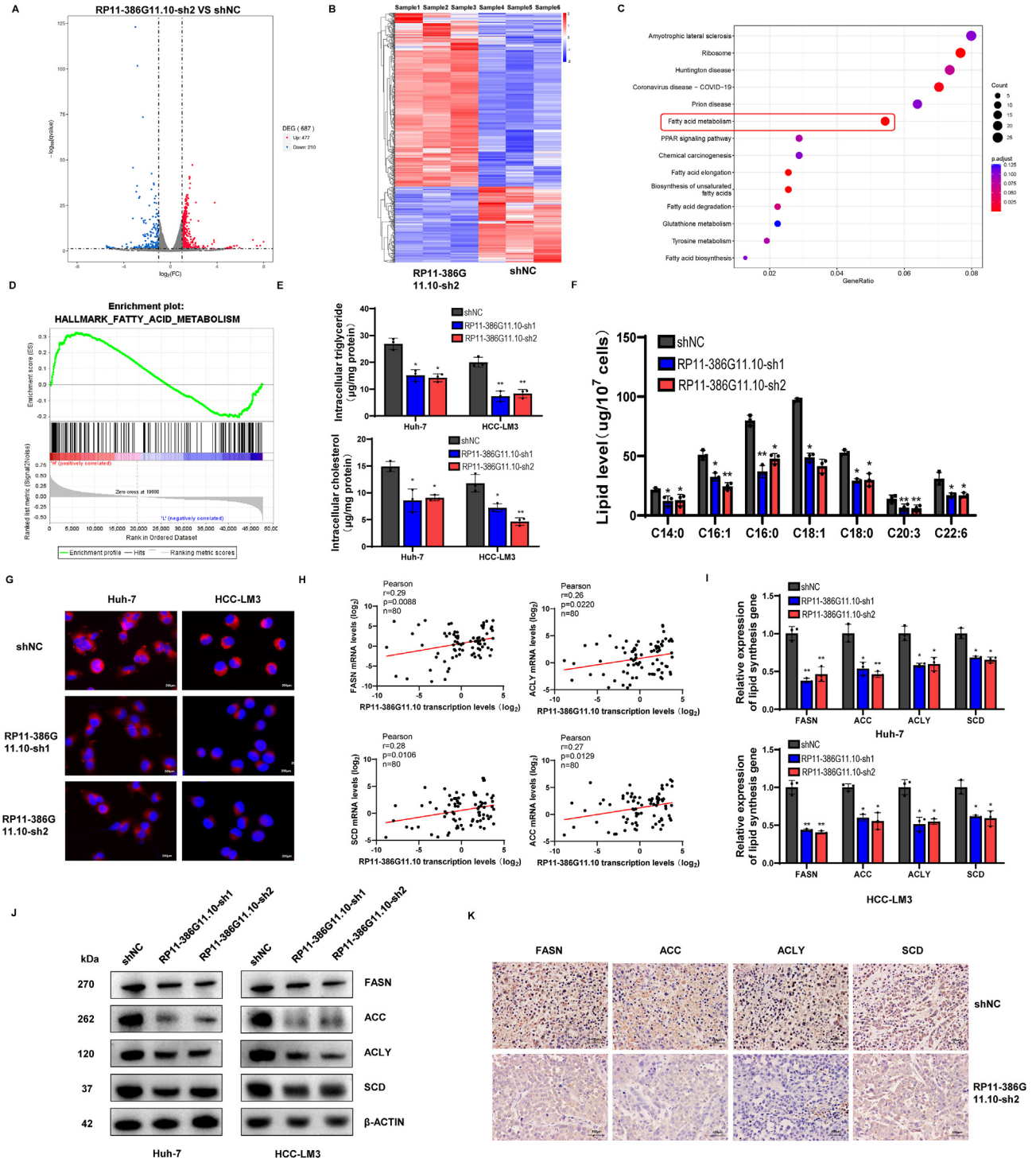

Figure 3: RP11-386G11.10 promotes lipid synthesis in HCC. **A** Volcano plot showed the sum of expression levels of genes affected by RP11-386G11.10 knockdown. **B** Heatmap showed differential expression of genes across all samples. **C** Bubble plot showing enriched pathways for mRNA expression affected by RP11-386G11.10 knockdown. **D** Positive enrichment for the gene signature associated fatty acid metabolism between the low and high RP11-386G11.10 expression groups of TCGA dataset. **E** Measurement of intracellular triglyceride and cholesterol content in Huh7 and HCC-LM3 cells transfected with shHRLL1. **F** The intracellular fatty acids of Huh-7 cells transfected with shHRLL1 analyzed by GC–MS. **G** Intracellular lipids in Huh7 and HCC-LM3 cells transfected with shHRLL1 measured by double staining with Nile Red and Hoechst. Magnification, 400 × . **H** Pearson correlation analysis of RP11-386G11.10 and FASN, ACLY, ASCD, ACC in 80 HCC tissue samples. **I, J** In the HCC cells with RP11-386G11.10 knockdown, the mRNA and protein levels of related lipogenic enzymes were significantly reduced. **K** In the HCC samples with RP11-386G11.10 knockdown, the expression of lipid synthase-related proteins was determined by IF analysis. $*p < 0.05$, $**p < 0.01$, $***p < 0.001$.

 © 2022 The Author(s). Published by Elsevier GmbH. This is an open access article under the CC BY-NC-ND license (http://creativecommons.org/licenses/by-nc-nd/4.0/).

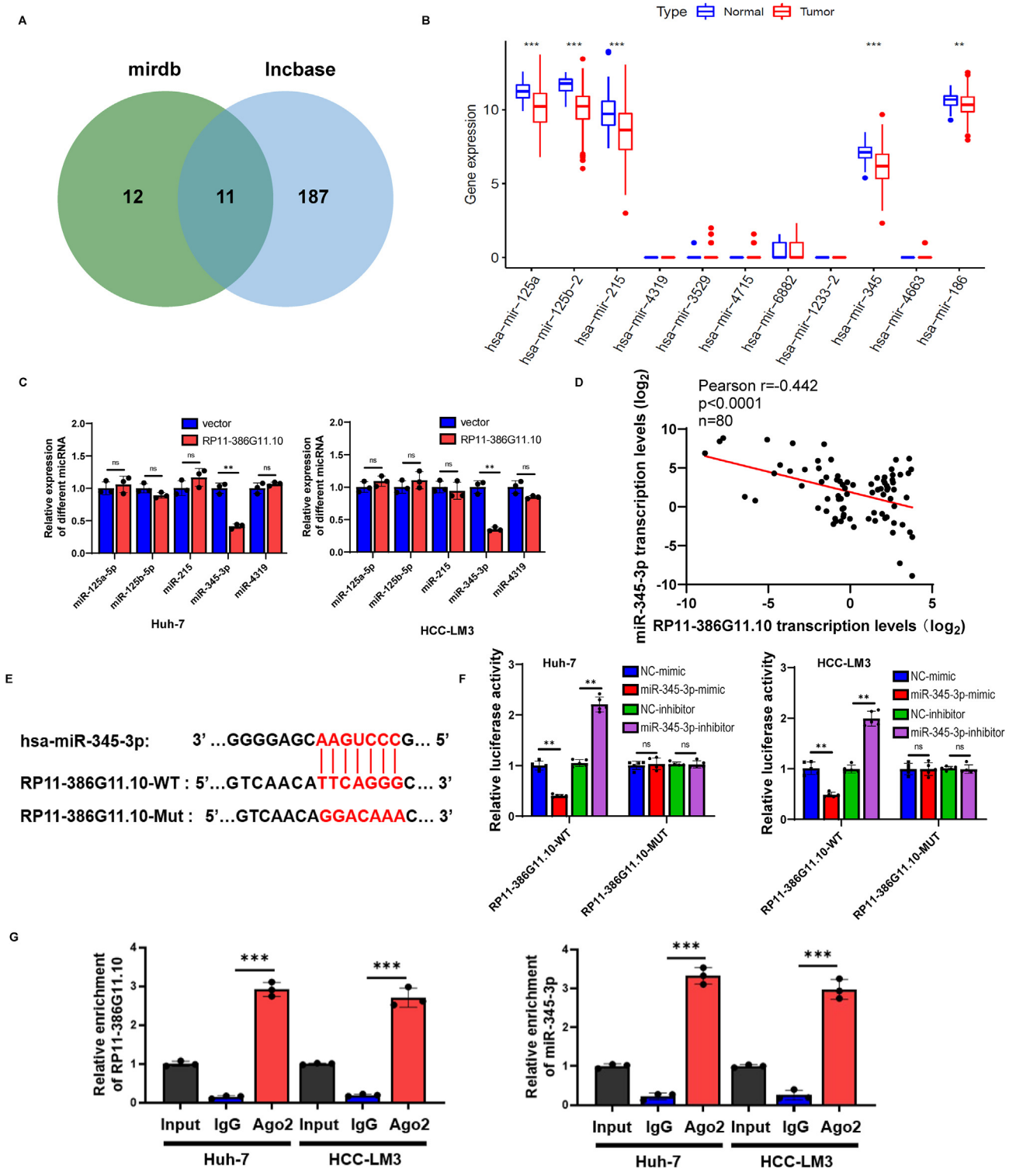

Figure 4: RP11-386G11.10 directly binds to miR-345−3p and negatively regulates miR-345−3p expression. **A** Bioinformatics analysis of potential target genes is performed by prediction software (mirdb, lncbase). **B** Target miRNA expression in HCC tumors and non-tumor tissues in the TCGA database. **C** qRT-PCR showed target miRNAs expression in RP11-386G11.10 overexpressing HCC cells. **D** Pearson correlation analysis of RP11-386G11.10 and miR-345−3p in 80 HCC tissue samples. **E** Schematic diagram of the potential binding site between RP11-386G11.10 and miR-345−3p. **F, G** Dual luciferase reporter gene detection and RIP experiment confirmed the interaction between RP11-386G11.10 and miR-345−3p. $*p < 0.05$, $**p < 0.01$, $***p < 0.001$.

 © 2022 The Author(s). Published by Elsevier GmbH. This is an open access article under the CC BY-NC-ND license (http://creativecommons.org/licenses/by-nc-nd/4.0/).

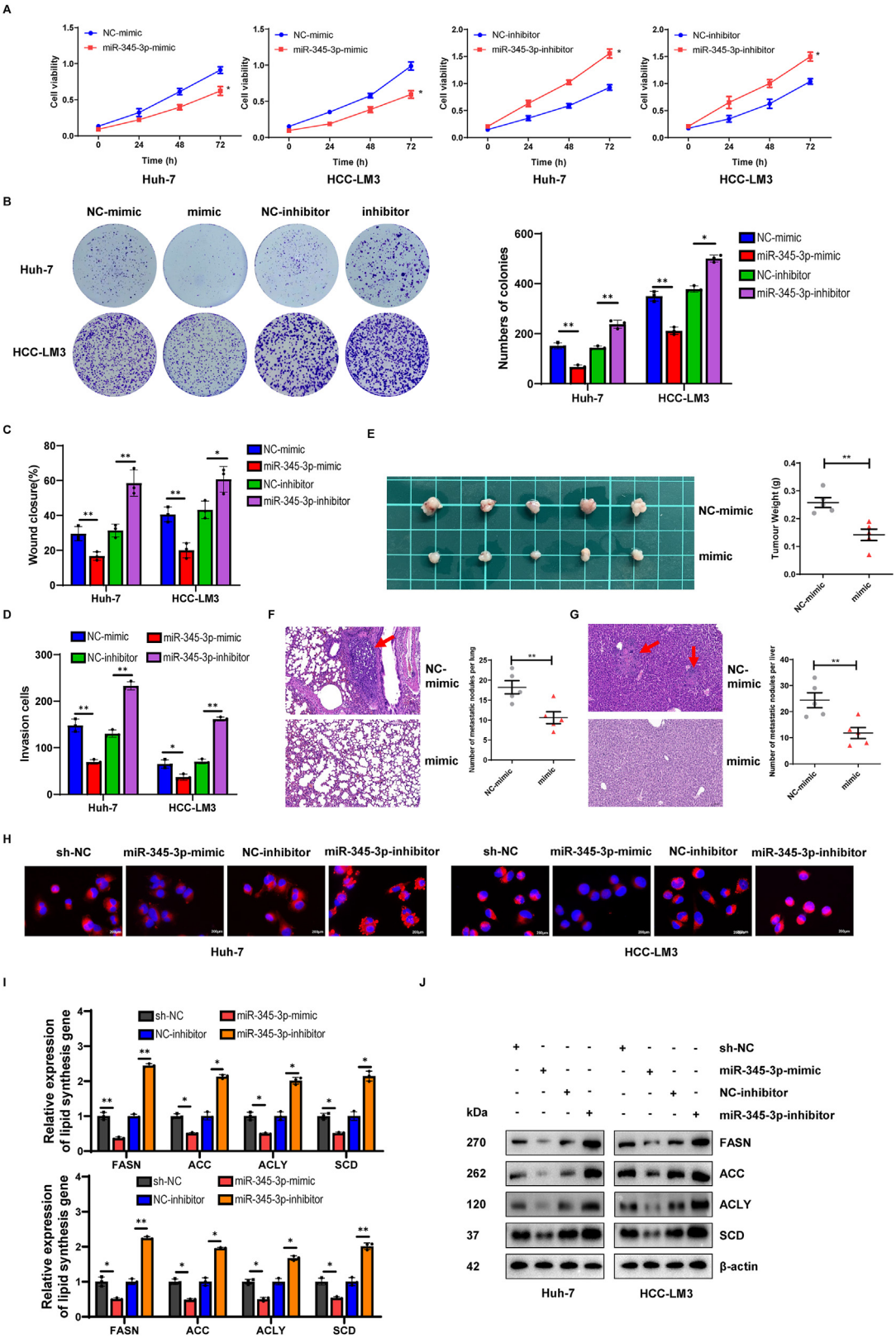

Figure 5: MiR-345−3p inhibits proliferation and metastasis and lipid synthesis in HCC. **A, B** RP11-386G11.10 inhibited HCC cell proliferation. **C, D** RP11-386G11.10 inhibited the migration and invasion ability of HCC cells. **E** A xenograft model established from control or miR-345−3p overexpressed HCC-LM3 cells, and assess the weight of the anatomical tumor. **F, G** HE staining showed miR-345−3p overexpression reduced the lung and liver metastasis in the nude mice. Magnification, 100 × . **H** The intracellular lipids were measured in Huh7 and HCC-LM3 cells overexpressing miR-345−3p by double staining with Nile Red and Hoechst. Magnification, 400 × . **I, J** Lipogenic enzymes mRNA and protein levels in miR-345−3p overexpressing or knocking down HCC cells. $*p < 0.05$, $**p < 0.01$, $***p < 0.001$.

 © 2022 The Author(s). Published by Elsevier GmbH. This is an open access article under the CC BY-NC-ND license (http://creativecommons.org/licenses/by-nc-nd/4.0/).

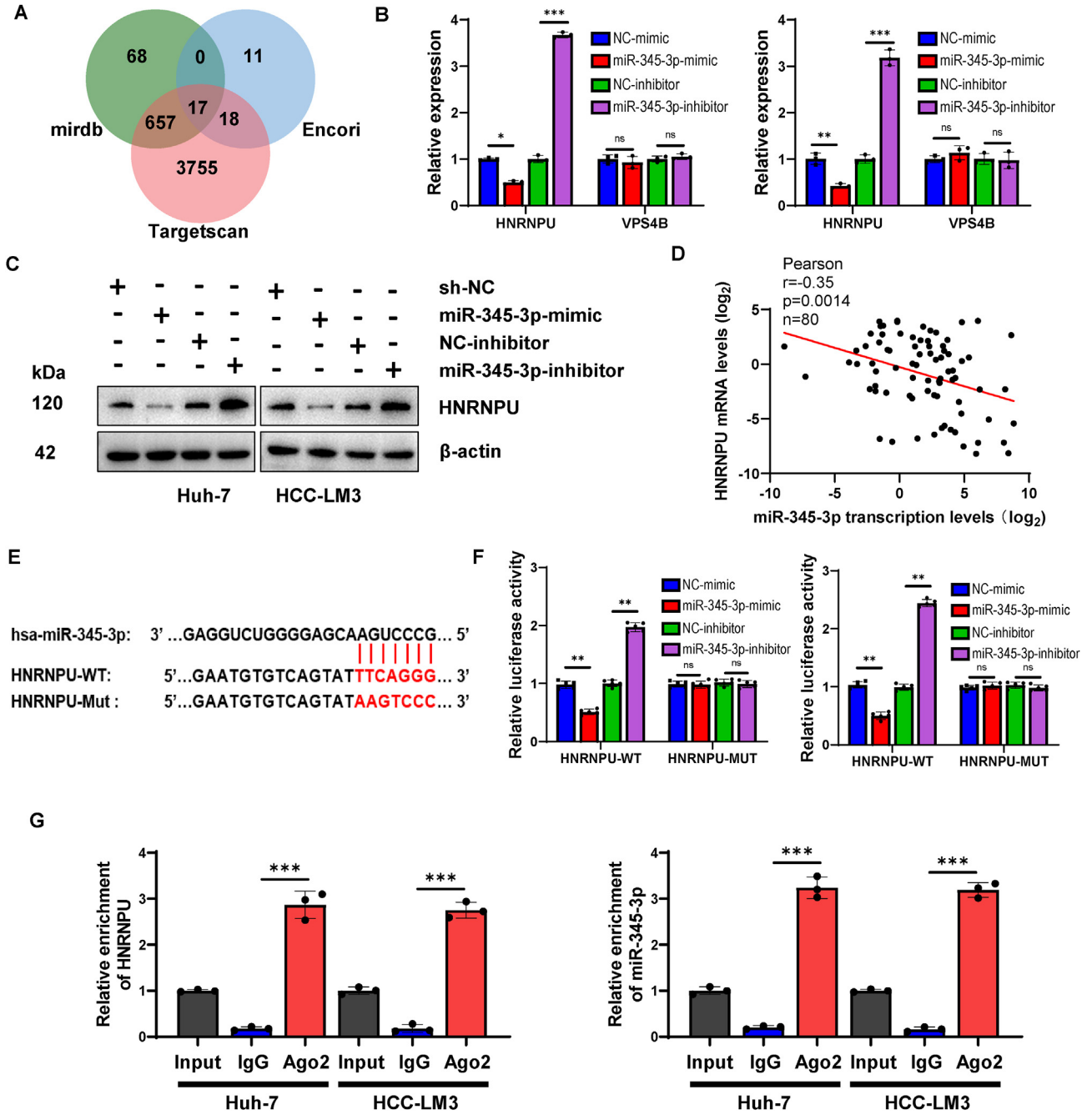

Figure 6: MiR-345−3p directly binds to HNRNPU and negatively regulates HNRNPU expression. **A** Prediction software (mirdb, encori and targetscan) screened possible downstream targets of miR-345−3p. **B** HNRNPU and VPS4B mRNA expression in miR-345−3p overexpressing or knocking down Huh-7 and HCC-LM3 cells. **C** The expression of HNRNPU protein levels miR-345−3p overexpressing or knocking down Huh-7 and HCC-LM3 cells. **D** Pearson correlation analysis of miR-345−3p and HNRNPU in 80 HCC tissue samples. **E** Schematic diagram of potential binding sites between miR-345−3p and HNRNPU. **F, G** Dual luciferase reporter gene and RIP test confirmed the interaction between miR-345−3p and HNRNPU. $*p < 0.05$, $**p < 0.01$, $***p < 0.001$.

as FASN, ACC, ACLY, and SCD in HCC cells (Figure 3I—J). In addition, the expression of other related genes involved in lipid uptake, synthesis, β-oxidation and export showed no significant changes (Fig. S2H). In RP11-386G11.10-overexpressing cells, the opposite alterations in lipid metabolism described above were observed (Figs. S2F—J). IHC analysis of subcutaneous tumours in nude mice showed that knocking down RP11-386G11.10 reduced the protein expression of FASN, ACC, ACLY, SCD and other genes in vivo (Figure 3K). In summary, our results showed that RP11-386G11.10 promotes lipid accumulation in HCC cells.

3.4. The lncRNA RP11-386G11.10 negatively regulates miR-345-3p by acting as a ceRNA

LncRNAs regulate cell biological processes through a variety of distinct mechanisms, and most lncRNAs perform their functions by acting as molecular sponges for miRNAs. Therefore, we hypothesized that

 © 2022 The Author(s). Published by Elsevier GmbH. This is an open access article under the CC BY-NC-ND license (http://creativecommons.org/licenses/by-nc-nd/4.0/).

RP11-386G11.10 may also interact with miRNAs as a ceRNA in HCC. The bioinformatics databases miRDB and LncBase were used to predict the possible interactions between RP11-386G11.10 and miRNAs, and RP11-386G11.10 was predicted to potentially regulate 11 miRNAs (Figure 4A). Analysis of public TCGA datasets showed that the expression of 5 miRNAs was significantly reduced in HCC tissues compared with the paired nontumour tissues (Figure 4B). After RP11-386G11.10 overexpression or knockdown, the expression of miR-345-3p expression exhibited the most obvious change (Figure 4C, Fig. S3A). In addition, Pearson analysis of the 80 HCC tissues showed that the expression of RP11-386G11.10 and miR-345-3p was significantly negatively correlated ($r = -0.44$, $p < 0.001$) (Figure 4D), indicating that RP11-386G11.10 is likely to be the ceRNA of miR-345-3p. To confirm the above speculation, we used miRNA mimics/inhibitors to upregulate/knock down the expression of mi-345-3p respectively (Fig. S3B), and constructed WT and MUT RP11-386G11.10 reporter plasmids (Figure 4E). The results of the dual luciferase reporter assay showed that the relative luciferase activity of RP11-386G11.10-WT cells with miR-345-3p overexpression was significantly reduced compared with that of control cells, while knocking down miR-345-3p significantly increased the relative luciferase activity in RP11-386G11.10-WT cells (Figure 4F). In contrast, no such changes were detected in RP11-386G11.10-MUT cells (Figure 4F). In addition, the RIP assay showed that RP11-386G11.10 and mi-345-3p bound to the anti-Ago2 antibody in the precipitated complexes, but did not bind to the IgG control (Figure 4G). Therefore, our results showed that RP11-386G11.10 contains a binding site for miR-345-3p and actes as a ceRNA to negatively regulate miR-345-3p.

3.5. MiR-345-3p inhibits HCC progression

Given that RP11-386G11.10 may act through sponging miR-345-3p, we further studied the biological functions of miR-345-3p. Our results showed that miR-345-3p overexpression inhibited while miR-345-3p knockdown promoted cell proliferation, invasion and migration abilities of HCC cells (Figure 5A–D, Fig. S3C). We next used subcutaneous xenograft, tail vein injection and intrasplenic injection models to explore the role of miR-345-3p in vivo. Both the volume and weight of tumours were significantly reduced in the miR-345-3p overexpression group (Figure 5E). In tail vein injection and intrasplenic injection models, miR-345-3p knockdown enhanced lung and liver metastasis nodules (Figure 5F–G). In summary, these results indicated that miR-345-3p inhibits the proliferation and metastasis of HCC cells in vitro and in vivo.

3.6. miR-345-3p inhibits lipid synthesis in HCC

We verified the interaction between RP11-386G11.10 and miR-345-3p, which suggested that miR-345-3p might also affect lipid synthesis in HCC. The results of Nile Red staining and measurement of triglyceride and cholesterol levels in HCC cells showed that overexpression/knockdown of miR-345-3p inhibited/promoted lipid accumulation in HCC cells respectively (Figure 5H, Fig. S3D). The qRT-PCR and western blot results showed that the expression of anabolic genes was down-regulated/upregulated with miR-345-3p overexpression/knockdown respectively (Figure 5I, Figure 5J). The above results indicate that miR-345-3p can delay the progression of HCC and inhibit lipid anabolism.

3.7. HNRNPU is the direct target gene of miR-345-3p

To clarify the direct target genes of miR-345-3p, we used bioinformatics techniques to predict 17 target genes potentially involved in the initiation and development of HCC (Figure 6A), among which only vacuolar protein sorting 4 homolog B (VPS4B) and HNRNPU have been reported to promote the development of HCC. The qRT-PCR and western blot results showed that miR-345-3p overexpression/knockdown could downregulate/upregulate the HNRNPU mRNA and protein expression, while VPS4B expression did not change significantly (Figure 6B, Figure 6C). Pearson correlation analysis of the 80 HCC tissues showed that the expression of miR-345-3p was negatively correlated with the expression of HNRNPU ($r = 0.30$, $p = 0.006$) (Figure 6D). Then, to clarify whether HNRNPU is directly regulated by miR-345-3p, we constructed WT and MUT HNRNPU plasmids and found that miR-345-3p mimic transfection significantly reduced the relative luciferase activity of HNRNPU-WT cells, while miR-345-3p inhibitor transfection showed the opposite effect (Figure 6E, Figure 6F). In contrast, no such changes were detected in HNRNPU-MUT cells (Figure 6F). Additionally, the RIP assay results showed that miR-345-3p and HNRNPU bound to the anti-Ago2 antibody in the precipitated complexes, but did not bind to the IgG control (Figure 6G). The above results indicated that miR-345-3p can bind to the target site in HNRNPU and regulate HNRNPU directly.

3.8. The lncRNA RP11-386G11.10 promotes HCC cell growth and metastasis through the miR-345-3p/HNRNPU axis

As previously reported in the literature, HNRNPU promotes the proliferation and metastasis of HCC cells by promoting lipid synthesis [18]. HNRNPU was highly expressed in HCC and correlated with poor prognosis, as shown by analysis of the TCGA-LIHC dataset (Fig. S4A, Fig. S4B). To clarify whether RP11-386G11.10 regulates the progression of HCC and lipid anabolism in HCC cells through the miR-345-3p/HNRNPU axis, we transferred the miR-345−3p inhibitor or HNRNPU plasmid into RP11-386G11.10 knockdown HCC cells. HNRNPU expression was reduced by knockdown of RP11-386G11.10 and, as anticipated, this inhibition was reversed by the miR-345−3p inhibitor (Fig. S4C). The results showed that both miR-345−3p knockdown and HNRNPU overexpression reversed the RP11-386G11.10 knockdown-induced decreases in the proliferation, migration and invasion abilities of HCC cells (Figure 7B–E, Fig. S4D). We then transferred the miR-345-3p inhibitor and HNRNPU plasmid into RP11-386G11.10 knockdown cells and implanted these cells into BALB/c nude mice by subcutaneous injection. MiR-345-3p inhibition or HNRNPU overexpression reversed the significant reductions in tumour volume and weight in the RP11-386G11.10-sh2 group, compared with the shNC group (Figure 6F). These results indicated that RP11-386G11.10 acts as a ceRNA of miR-345-3p to regulate the expression of HNRNPU, leading to the development of HCC.

3.9. The RP11-386G11.10/miR-345-3p/HNRNPU axis-mediated lipid metabolic reprogramming is the cause of HCC progression

Then, we observed that the reduction in lipid levels caused by RP11-386G11.10 knockdown in tumour sections was reversed by miR-345-3p inhibitor transfection and overexpression of HNRNPU (Figure 7G, Figure 7H). Additionally, both miR-345-3p suppression and HNRNPU overexpression reversed the RP11-386G11.10 knockdown-induced downregulation of the mRNA and protein expression of key lipid synthesis genes such as FASN, ACC, ACLY, and SCD (Figure 7I, Figure 7J). The same changes were also observed in HCC cell lines (Figs. S4E–H). These results indicated that RP11-386G11.10 promotes the growth and metastasis of HCC cells through lipid anabolism regulated by the miR-345-3p/HNRNPU axis.

 © 2022 The Author(s). Published by Elsevier GmbH. This is an open access article under the CC BY-NC-ND license (http://creativecommons.org/licenses/by-nc-nd/4.0/).

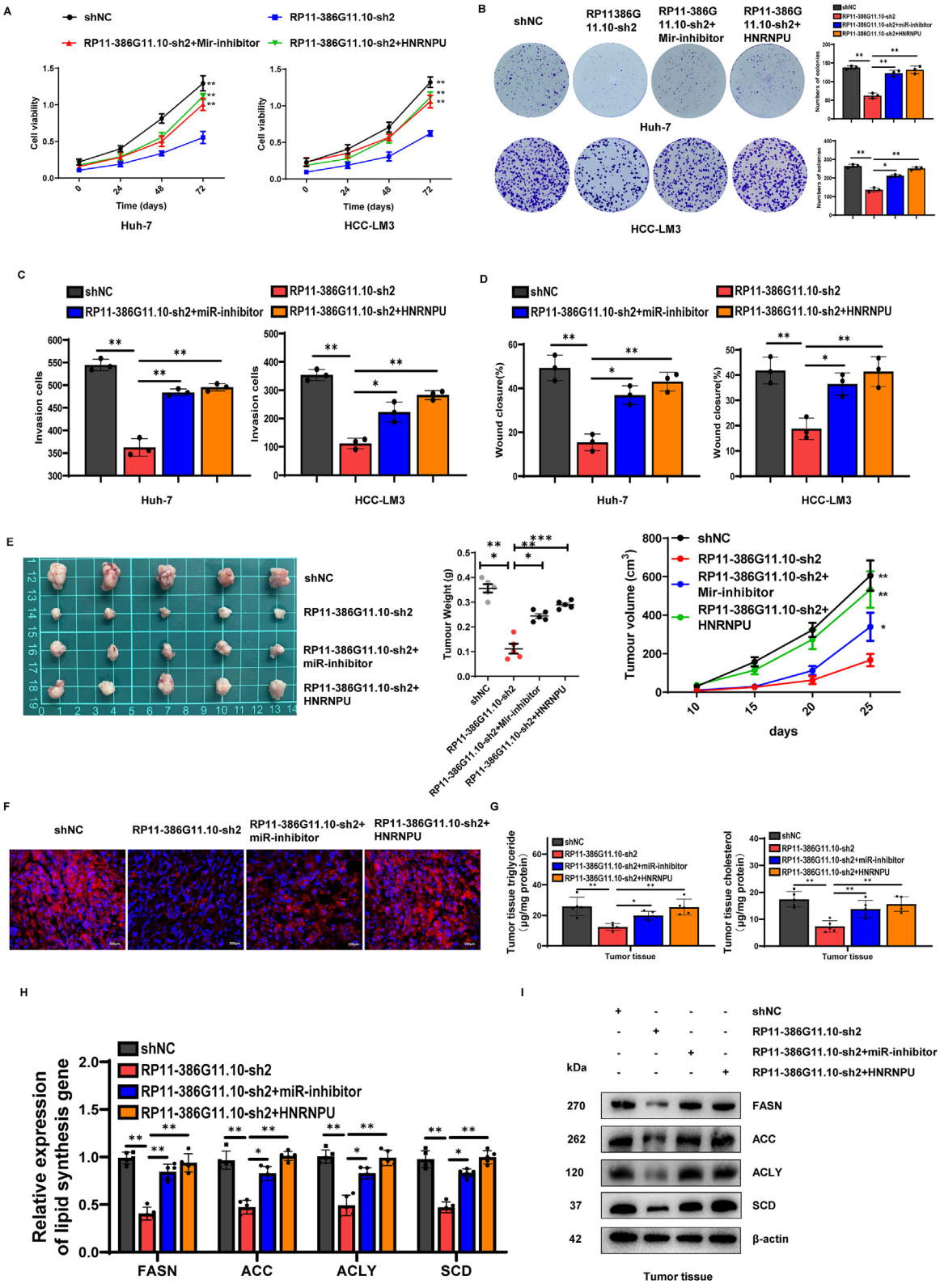

Figure 7: RP11-386G11.10 promotes cell growth and metastasis and lipid synthesis in HCC through the miR-345−3p/HNRNPU axis. **A, B** The proliferation ability of HCC cells was assessed by CCK-8 and colony formation assays. **C** The wound healing assay showed the migration ability of HCC cells. **D** The Transwell invasion assay with Matrigel showed the cell invasion ability. **E** Tumour growth curves from the xenograft model established with cotransfected HCC-LM3 cells and evaluation of the weights of the excised tumours. **F** The intracellular lipid content was evaluated in the tumour tissues described in F by double staining with Nile Red and Hoechst. Magnification, 200×. **G** The triglyceride and cholesterol contents were measured in the tumour tissues described in F. **H, I** Lipogenic enzyme mRNA and protein levels were measured in the tumour tissues described in F. $^{*}p < 0.05$, $^{**}p < 0.01$, $^{***}p < 0.001$.

 © 2022 The Author(s). Published by Elsevier GmbH. This is an open access article under the CC BY-NC-ND license (http://creativecommons.org/licenses/by-nc-nd/4.0/).

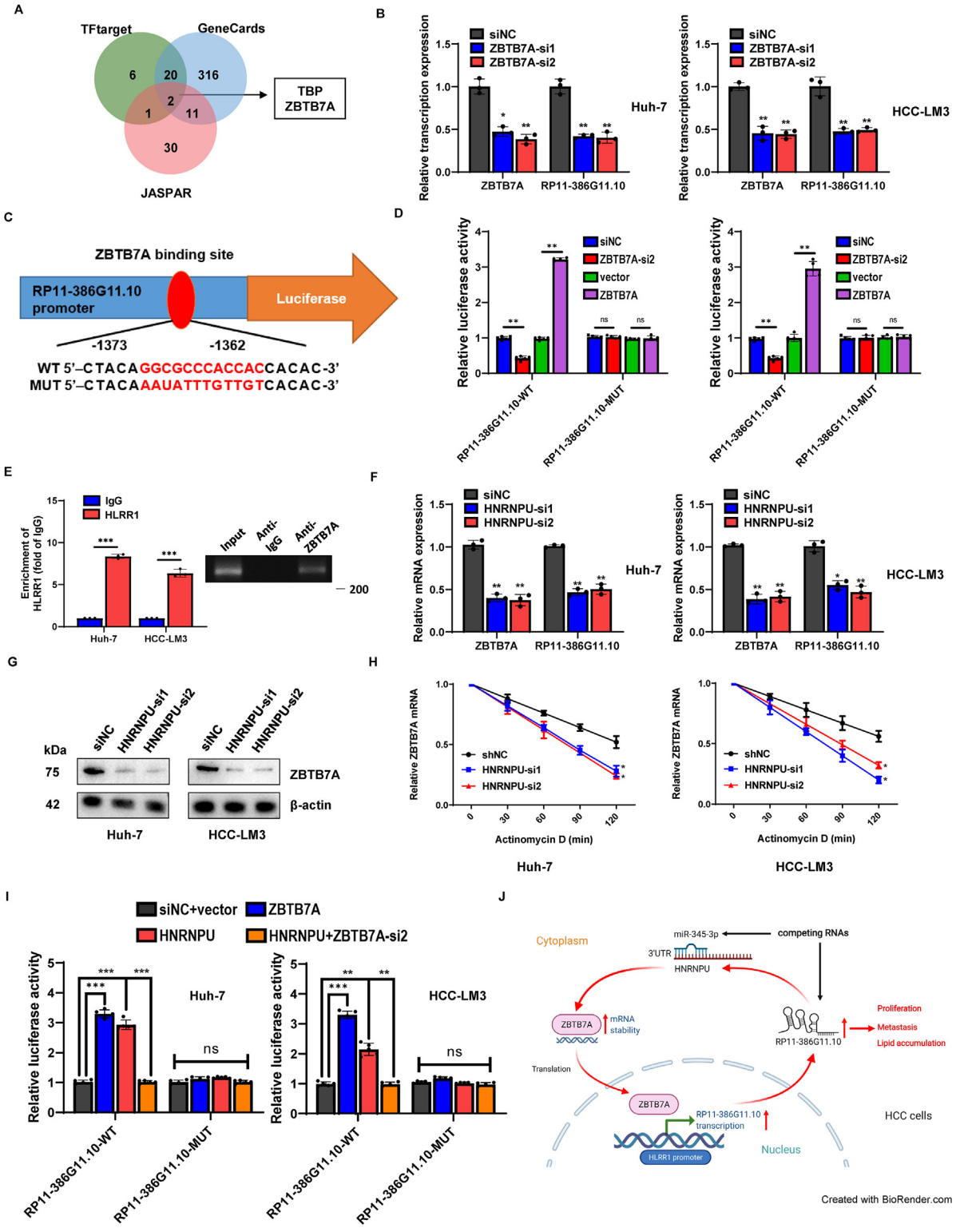

Figure 8: RP11-386G11.10 is directly regulated by the transcription factor ZBTB7A. **A** Transcription factors that may regulate the transcription of RP11-386G11.10 were identified by prediction databases (tfTarget, GeneCards and JASPAR). **B** The expression levels of ZBTB7A and RP11-386G11.10 in HCC cells with ZBTB7A knockdown were verified by qRT-PCR. **C** The binding sequence of ZBTB7A and RP11-386G11.10 predicted from the JASPAR database. **D** The results of the dual luciferase reporter assay confirmed the interaction between ZBTB7A and RP11-386G11.10. **E** The CHIP assay results confirmed the direct binding between ZBTB7A and the RP11-386G11.10 promoter region. **F** The expression levels of ZBTB7A and RP11-386G11.10 in HCC cells with HNRNPU knockdown were verified by qRT-PCR. **G** The protein expression levels of ZBTB7A in HCC cells with HNRNPU knockdown. **H** Changes in ZBTB7A mRNA stability after actinomycin D treatment of Huh-7 and HCC-LM3 cells. **I** The effects of different transfectants on the interaction between ZBTB7A and the RP11-386G11.10 promoter were verified by a luciferase reporter assay in HCC cells. **J**. A model of the regulatory mechanisms of RP11-386G11.10 in HCC. $*p < 0.05$, $**p < 0.01$, $***p < 0.001$.

 © 2022 The Author(s). Published by Elsevier GmbH. This is an open access article under the CC BY-NC-ND license (http://creativecommons.org/licenses/by-nc-nd/4.0/).

3.10. ZBTB7A is a transcription factor of the lncRNA RP11-386G11.10

Finally, to clarify the overexpression of RP11-386G11.10 in HCC, we used the hTFtarget, geneCARDS and UCSC Genome Browser databases to predict that TATA-box binding protein (TBP) and ZBTB7A may be transcription factors regulating RP11-386G11.10 (Figure 8A), and we found that both TFs were overexpressed in HCC tissues (Fig. S5A). Knocking down ZBTB7A significantly reduced RP11-386G11.10 expression (Figure 8B). However, RP11-386G11.10 expression did not change significantly after TBP knockdown (Fig. S5B). To verify that ZBTB7A exerted a transcriptional regulatory effect on RP11-386G11.10, we constructed WT and MUT RP11-386G11.10 plasmids based on the sequence of the RP11-386G11.10 and ZBTB7A binding site (GGCGCCCACCAC) predicted by promoter analysis tools (UCSC and JASPAR) (Figure 8C). Then, we constructed ZBTB7A overexpression models with HCC cells and found that ZBTB7A overexpression significantly increased the relative luciferase activity of RP11-386G11.10-WT cells, while ZBTB7A knockdown showed the opposite effect (Figure 8D, Fig. S5D). In contrast, no such changes were detected in RP11-386G11.10-MUT cells (Figure 8D). In addition, the results of ChIP-qPCR further confirmed that ZBTB7A directly binds to the promoter region of RP11-386G11.10 (Figure 8E).

3.11. HNRNPU forms a positive feedback loop that promotes the expression of the lncRNA RP11-386G11.10 by activating ZBTB7A

Based on the findings that RP11-386G11.10, ZBTB7A and HNRNPU were highly expressed in HCC, and that there were strong correlations between the three (Fig. S5C), we hypothesized that the strong promotive effects of RP11-386G11.10 on HCC progression and lipid synthesis are due to a potential positive feedback loop. HNRNPU knockdown reduced the mRNA and protein expression levels of ZBTB7A and mRNA expression levels of RP11-386G11.10 (Figure 8F—G). As reported, HNRNPU promotes cancer progression by stabilizing downstream target gene mRNA [29—32], and we observed that the stability of ZBTB7A mRNA decreases after HNRNPU knockdown in HCC cells as expected (Figure 8H). In addition, HNRNPU overexpression increased the relative luciferase activity of RP11-386G11.10-WT cells (Figure 8I). ZBTB7A knockdown reversed the effect of HNRNPU overexpression on RP11-386G11.10-WT cells, but no significant changes were observed in RP11-386G11.10-MUT cells, which indicated that HNRNPU promoted the binding of ZBTB7A to the RP11-386G11.10 promoter region (Figure 8I). Additionally, overexpression of either ZBTB7A or HNRNPU enhanced RP11-386G11.10 expression, and this effect was reversed by knockdown of ZBTB7A, with the same trend observed in the luciferase reporter gene detection (Fig. S5D). The above results indicated that HNRNPU stabilized ZBTB7A mRNA to promote HCC progression and lipid accumulation by forming a positive feedback loop that activates RP11-386G11.10.

4. DISCUSSION

Tumour metabolism is complex, and with the exception of the well-known Warburg effect, the impact of other metabolic pathways on tumour progression remains unclear [33]. Recently, accumulating evidence has shown that lipid metabolic reprogramming is involved in tumour growth and metastasis. Dysregulation of lipid synthesis has been considered an essential carcinogenic event in human HCC [34]. Lipids are needed as membrane components, as signalling molecules, and for energy storage in cancer cells. In cancer cells, almost all lipids are produced through de novo synthesis to support the rapid growth of tumours, even if the extracellular lipid supply is sufficient [35]. Multiple mechanisms help to increase de novo lipid synthesis in cancer cells, and most of these mechanisms involve upregulation of key lipogenic enzymes [35]. Reports indicate that lipogenic enzymes such as FASN, ACLY, ACC and SCD are abnormally overexpressed in diverse human solid tumours, including HCC [36,37]. In addition, blocking FA biosynthetic pathways has been shown to inhibit cancer cell growth, and several potential targets in these pathways could serve as effective drug targets as part of HCC therapeutic strategies [38] Therefore, a better understanding of lipid metabolic reprogramming in HCC cells may facilitate the development of promising therapeutic strategies for this malignant tumour. Notably, lncRNAs have been shown to play an important role in regulating lipogenesis in cells, but there are few reports of lncRNAs regulating lipid anabolism in HCC.

Antisense lncRNAs are known to bind to mRNAs with complementary sequences to it (sense RNAs) and inhibit their translation [39]. Since RP11-386G11.10 shares the same locus with the TUBA1B gene, we constructed knockdown models of RP11-386G11.10 or TUBA1B to rule out the possibility that they affected each other (Figure 2A, Fig. S1H). Our results showed that knockdown of either TUBA1B or RP11-386G11.10 did not alter the expression of the other (Figs. S1G—I).

ceRNAs have been proved to constitute a common and essential mechanism for the regulation of HCC progression. Although the ceRNA mechanism has not been reported in lipid metabolism in HCC, it has been confirmed to play a role in lipid metabolism in nonalcoholic fatty liver and steatohepatitis [40,41]. In subsequent studies, we proved the endogenous interaction between RP11-386G11.10 and miR-345-3p through bioinformatics analysis and luciferase reporter and RIP assays. The effects of miR-345-3p on tumour suppression and lipid synthesis in HCC were observed, and RP11-386G11.10 was confirmed to act as a miR-345-3p sponge to promote HCC cell proliferation, invasion and lipid synthesis.

Our results showed that RP11-386G11.10 positively regulates HNRNPU expression by sponging miR-345-3p in HCC. Importantly, our co-transfection experiment proved that the changes in the RP11-386G11.10, miR-345-3p and HNRNPU expression levels were related to the proliferation and metastasis activities of HCC cells and to the activity of lipid metabolism pathways, suggesting that the RP11-386G11.10/miR-345-3p/HNRNPU axis promotes lipid synthesis and mediates the progression of HCC. Although HNRNPU may not be the only target gene of RP11-386G11.10, our results demonstrated that HNRNPU is an important downstream target in RP11-386G11.10-mediated HCC development.

ZBTB7A is a common transcription factor in cancer [23]. We proved that ZBTB7A is a positive transcription factor of RP11-386G11.10. Our results indicated activation of ZBTB7A activated RP11-386G11.10 to form a positive feedback loop, which may have crucial implications for HCC progression and lipid accumulation caused by high RP11-386G11.10 expression.

In summary, we proposed a new mechanism of lncRNA-mediated lipid metabolic reprogramming in the progression of HCC, and expanded the understanding of lncRNA-mediated regulation of metabolic homeostasis in HCC. Moreover, since lipogenesis is not common in normal cells, methods targeting lipogenic enzymes and their signalling cascades are very promising for the development of innovative drugs for cancer treatment [42]. From this perspective, our research provided possible prognostic indicators for HCC and paved the way for the development of new HCC therapeutic drugs and strategies.

 © 2022 The Author(s). Published by Elsevier GmbH. This is an open access article under the CC BY-NC-ND license (http://creativecommons.org/licenses/by-nc-nd/4.0/).

AUTHOR CONTRIBUTION STATEMENT

Conception and design: K.X, P.X; Development of methodology: K.X, P.X, X.G, X.Z, Z.C, H.Z, Y.Y, Y.L; Collection and acquisition of data: S.M, J.L, G.Y, Y.L, Y.Y, Y.C; Analysis of data: K.X, P.X, X.G, H.Z, J.L,Y.Y, Y.L, Y.G; Writing, review, and/or revision of the manuscript: K.X, P.X, X.G, X.Z, Z.C, Z.Z, YF.Y. All authors read and approved the final manuscript.

ETHICS STATEMENT

The study was approved by the Hospital's Protection of Human Subjects Committee (KELUN 2018010). All the animal experiments were conducted strictly according to the Guide for the Care and Use of Laboratory Animals and approved by the Laboratory Animal Ethics Committee, Zhongnan Hospital of Wuhan University (Hubei province, China).

DATA AVAILABILITY

The data that support the findings of this study are available from the corresponding author upon reasonable request.

FUNDING STATEMENT

Our work was supported by Research Fund of the Health Commission of Hubei Province (WJ2021M255); Cancer research and translational platform project of Zhongnan Hospital of Wuhan University (ZLYNXM202004); Translational medicine and interdisciplinary research joint fund project of Zhongnan Hospital of Wuhan University (ZNJC201918); grant from the National Key Research and Development Program of China (SQ2019YFC200078/02).

ACKNOWLEDGMENTS

We acknowledge and appreciate our colleagues Weijie Ma and Xi Chen for their valuable suggestions and technical assistance for this study.

CONFLICT OF INTEREST

The authors declare that they have no competing interests.

APPENDIX A. SUPPLEMENTARY DATA

Supplementary data to this article can be found online at https://doi.org/10.1016/j.molmet.2022.101540.

ABBREVIATIONS

AGO2	Argonaute2
ceRNAs	Competing endogenous RNAs
ChIP	Chromatin immunoprecipitation
DMEM	Dulbecco's modified eagle's medium
FISH	Fluorescence in situ hybridization
HCC	Hepatocellular carcinoma
RP11-386G11.10	LncRNA hepatocarcinoma lipid reprogramming regulator 1
HNRNPU	Heterogeneous nuclear ribonucleoprotein U
lncRNA	Long noncoding RNA
miRNAs	MicroRNAs
RIP	RNA immunoprecipitation
shRNA	Short hairpin RNA
TCGA-LIHC	The Cancer Genome Atlas-Liver Hepatocellular Carcinoma
VPS4B	Vacuolar protein sorting 4 homolog B

REFERENCES

[1] Park, J.W., Chen, M., Colombo, M., Roberts, L.R., Schwartz, M., Chen, P.J., et al., 2015. Global patterns of hepatocellular carcinoma management from diagnosis to death: the BRIDGE Study. Liver International 35(9):2155–2166.

[2] Forner, A., Reig, M., Bruix, J., 2018. Hepatocellular carcinoma. Lancet 391(10127):1301–1314.

[3] Sim, H.W., Knox, J., 2018. Hepatocellular carcinoma in the era of immunotherapy. Current Problems in Cancer 42(1):40–48.

[4] European Association For The Study Of The, L., European Organisation For, R., Treatment Of, C., 2012. EASL-EORTC clinical practice guidelines: management of hepatocellular carcinoma. Journal of Hepatology 56(4):908–943.

[5] Qian, X., Zhao, J., Yeung, P.Y., Zhang, Q.C., Kwok, C.K., 2019. Revealing lncRNA structures and interactions by sequencing-based approaches. Trends in Biochemical Sciences 44(1):33–52.

[6] Militello, G., Weirick, T., John, D., Doring, C., Dimmeler, S., Uchida, S., 2017. Screening and validation of lncRNAs and circRNAs as miRNA sponges. Briefings in Bioinformatics 18(5):780–788.

[7] Wang, Y., Yang, L., Chen, T., Liu, X., Guo, Y., Zhu, Q., et al., 2019. A novel lncRNA MCM3AP-AS1 promotes the growth of hepatocellular carcinoma by targeting miR-194-5p/FOXA1 axis. Molecular Cancer 18(1):28.

[8] Cao, J., Tang, Z., Su, Z., 2020. Long non-coding RNA LINC01426 facilitates glioblastoma progression via sponging miR-345-3p and upregulation of VAMP8. Cancer Cell International 20:327.

[9] Zeng, Q., Jin, F., Qian, H., Chen, H., Wang, Y., Zhang, D., et al., 2022. The miR-345-3p/PPP2CA signaling axis promotes proliferation and invasion of breast cancer cells. Carcinogenesis 43(2):150–159.

[10] Peng, W.X., Koirala, P., Mo, Y.Y., 2017. LncRNA-mediated regulation of cell signaling in cancer. Oncogene 36(41):5661–5667.

[11] Currie, E., Schulze, A., Zechner, R., Walther, T.C., Farese Jr., R.V., 2013. Cellular fatty acid metabolism and cancer. Cell Metabolism 18(2):153–161.

[12] Ward, P.S., Thompson, C.B., 2012. Metabolic reprogramming: a cancer hallmark even warburg did not anticipate. Cancer Cell 21(3):297–308.

[13] Ma, H.Y., Yamamoto, G., Xu, J., Liu, X., Karin, D., Kim, J.Y., et al., 2020. IL-17 signaling in steatotic hepatocytes and macrophages promotes hepatocellular carcinoma in alcohol-related liver disease. Journal of Hepatology 72(5):946–959.

[14] Yang, Q., Chen, X., Zhang, Y., Hu, S., Hu, F., Huang, Y., et al., 2021. The E3 ubiquitin ligase RNF5 ameliorates nonalcoholic steatohepatitis via ubiquitin-mediated degradation of HRD1. Hepatology 74(6):3018–3036.

[15] Xu, D., Wang, Z., Xia, Y., Shao, F., Xia, W., Wei, Y., et al., 2020. The gluconeogenic enzyme PCK1 phosphorylates INSIG1/2 for lipogenesis. Nature 580(7804):530–535.

[16] Wang, C., Tong, Y., Wen, Y., Cai, J., Guo, H., Huang, L., et al., 2018. Hepatocellular carcinoma-associated protein TD26 interacts and enhances sterol regulatory element-binding protein 1 activity to promote tumor cell proliferation and growth. Hepatology 68(5):1833–1850.

[17] Calvisi, D.F., Wang, C., Ho, C., Ladu, S., Lee, S.A., Mattu, S., et al., 2011. Increased lipogenesis, induced by AKT-mTORC1-RPS6 signaling, promotes development of human hepatocellular carcinoma. Gastroenterology 140(3):1071–1083.

[18] Xing, S., Li, Z., Ma, W., He, X., Shen, S., Wei, H., et al., 2019. DIS3L2 promotes progression of hepatocellular carcinoma via hnRNP U-mediated alternative splicing. Cancer Research 79(19):4923–4936.

 © 2022 The Author(s). Published by Elsevier GmbH. This is an open access article under the CC BY-NC-ND license (http://creativecommons.org/licenses/by-nc-nd/4.0/).

[19] Bi, H.S., Yang, X.Y., Yuan, J.H., Yang, F., Xu, D., Guo, Y.J., et al., 2013. H19 inhibits RNA polymerase II-mediated transcription by disrupting the hnRNP U-actin complex. Biochimica et Biophysica Acta 1830(10):4899–4906.
[20] Silva, F.P., Hamamoto, R., Furukawa, Y., Nakamura, Y., 2006. TIPUH1 encodes a novel KRAB zinc-finger protein highly expressed in human hepatocellular carcinomas. Oncogene 25(36):5063–5070.
[21] Zhang, B., Wang, H.Y., Zhao, D.X., Wang, D.X., Zeng, Q., Xi, J.F., et al., 2021. The splicing regulatory factor hnRNPU is a novel transcriptional target of c-Myc in hepatocellular carcinoma. FEBS Letters 595(1):68–84.
[22] Zhang, X., Xue, C., Lin, J., Ferguson, J.F., Weiner, A., Liu, W., et al., 2018. Interrogation of nonconserved human adipose lincRNAs identifies a regulatory role of linc-ADAL in adipocyte metabolism. Science Translational Medicine 10(446).
[23] Gupta, S., Singh, A.K., Prajapati, K.S., Kushwaha, P.P., Shuaib, M., Kumar, S., 2020. Emerging role of ZBTB7A as an oncogenic driver and transcriptional repressor. Cancer Letters 483:22–34.
[24] Di Palo, A., Siniscalchi, C., Mosca, N., Russo, A., Potenza, N., 2020. A novel ceRNA regulatory network involving the long non-coding antisense RNA SPACA6P-as, miR-125a and its mRNA targets in hepatocarcinoma cells. International Journal of Molecular Sciences 21(14).
[25] Zhou, J.P., Ren, Y.D., Xu, Q.Y., Song, Y., Zhou, F., Chen, M.Y., et al., 2020. Obesity-induced upregulation of ZBTB7A promotes lipid accumulation through SREBP1. BioMed Research International 2020:4087928.
[26] Xia, P., Zhang, H., Xu, K., Jiang, X., Gao, M., Wang, G., et al., 2021. MYC-targeted WDR4 promotes proliferation, metastasis, and sorafenib resistance by inducing CCNB1 translation in hepatocellular carcinoma. Cell Death & Disease 12(7):691.
[27] Ubhayasekera, S.J., Staaf, J., Forslund, A., Bergsten, P., Bergquist, J., 2013. Free fatty acid determination in plasma by GC-MS after conversion to Weinreb amides. Analytical and Bioanalytical Chemistry 405(6):1929–1935.
[28] Zhang, X., Yang, J., Guo, Y., Ye, H., Yu, C., Xu, C., et al., 2010. Functional proteomic analysis of nonalcoholic fatty liver disease in rat models: enoyl-coenzyme a hydratase down-regulation exacerbates hepatic steatosis. Hepatology 51(4):1190–1199.
[29] Alfano, L., Caporaso, A., Altieri, A., Dell'Aquila, M., Landi, C., Bini, L., et al., 2019. Depletion of the RNA binding protein HNRNPD impairs homologous recombination by inhibiting DNA-end resection and inducing R-loop accumulation. Nucleic Acids Research 47(8):4068–4085.
[30] Qu, J., Xiong, X., Hujie, G., Ren, J., Yan, L., Ma, L., 2021. MicroRNA-132-3p alleviates neuron apoptosis and impairments of learning and memory abilities in Alzheimer's disease by downregulation of HNRNPU stabilized BACE1. Cell Cycle 20(21):2309–2320.
[31] Weidensdorfer, D., Stohr, N., Baude, A., Lederer, M., Kohn, M., Schierhorn, A., et al., 2009. Control of c-myc mRNA stability by IGF2BP1-associated cytoplasmic RNPs. RNA 15(1):104–115.
[32] Yugami, M., Kabe, Y., Yamaguchi, Y., Wada, T., Handa, H., 2007. hnRNP-U enhances the expression of specific genes by stabilizing mRNA. FEBS Letters 581(1):1–7.
[33] Berndt, N., Eckstein, J., Heucke, N., Gajowski, R., Stockmann, M., Meierhofer, D., et al., 2019. Characterization of lipid and lipid droplet metabolism in human HCC. Cells 8(5).
[34] Yamashita, T., Honda, M., Takatori, H., Nishino, R., Minato, H., Takamura, H., et al., 2009. Activation of lipogenic pathway correlates with cell proliferation and poor prognosis in hepatocellular carcinoma. Journal of Hepatology 50(1):100–110.
[35] Chen, J., Ding, C., Chen, Y., Hu, W., Yu, C., Peng, C., et al., 2021. ACSL4 reprograms fatty acid metabolism in hepatocellular carcinoma via c-Myc/SREBP1 pathway. Cancer Letters 502:154–165.
[36] Menendez, J.A., Lupu, R., 2007. Fatty acid synthase and the lipogenic phenotype in cancer pathogenesis. Nature Reviews Cancer 7(10):763–777.
[37] Khwairakpam, A.D., Shyamananda, M.S., Sailo, B.L., Rathnakaram, S.R., Padmavathi, G., Kotoky, J., et al., 2015. ATP citrate lyase (ACLY): a promising target for cancer prevention and treatment. Current Drug Targets 16(2):156–163.
[38] Pope 3rd, E.D., Kimbrough, E.O., Vemireddy, L.P., Surapaneni, P.K., Copland 3rd, J.A., Mody, K., 2019. Aberrant lipid metabolism as a therapeutic target in liver cancer. Expert Opinion on Therapeutic Targets 23(6):473–483.
[39] Xin, M., Guo, Q., Lu, Q., Lu, J., Wang, P.S., Dong, Y., et al., 2021. Identification of Gm15441, a Txnip antisense lncRNA, as a critical regulator in liver metabolic homeostasis. Cell & Bioscience 11(1):208.
[40] Huang, P., Huang, F.Z., Liu, H.Z., Zhang, T.Y., Yang, M.S., Sun, C.Z., 2019. LncRNA MEG3 functions as a ceRNA in regulating hepatic lipogenesis by competitively binding to miR-21 with LRP6. Metabolism 94:1–8.
[41] Chen, X., Tan, X.R., Li, S.J., Zhang, X.X., 2019. LncRNA NEAT1 promotes hepatic lipid accumulation via regulating miR-146a-5p/ROCK1 in nonalcoholic fatty liver disease. Life Sciences 235:116829.
[42] Braig, S., 2018. Chemical genetics in tumor lipogenesis. Biotechnology Advances 36(6):1724–1729.

 © 2022 The Author(s). Published by Elsevier GmbH. This is an open access article under the CC BY-NC-ND license (http://creativecommons.org/licenses/by-nc-nd/4.0/).